Remote Sensing of Environment 205 (2018) 224–235

Contents lists available at ScienceDirect

Remote Sensing of Environment

journal homepage: www.elsevier.com/locate/rse

An airborne remote sensing case study of synthetic hydrocarbon detection using short wave infrared absorption features identified from marine-harvested macro- and microplastics

Shungudzemwoyo P. Garaba[a,*], Heidi M. Dierssen[a,b]

[a] Department of Marine Sciences, Avery Point Campus, University of Connecticut, 1080 Shennecossett Road, Groton, CT 06340, USA
[b] Institute of Material Science, Storrs Campus, University of Connecticut, 97 North Eagleville Road, Storrs, CT 06269-3136, USA

ARTICLE INFO

Keywords:
Spectral reflectance
Dry virgin plastic polymer
Hyperspectral remote sensing
AVIRIS
Marine-harvested microplastics
Macroplastics

ABSTRACT

The abundance and distribution of plastic debris in natural waters is largely unknown due to limited comprehensive monitoring. Here, optical properties of dry and wet marine-harvested plastic debris were quantified to explore the feasibility of plastic debris optical remote sensing in the natural environment. We measured the spectral reflectance of microplastics (< 5 mm) from the North Atlantic Ocean, macroplastics (> 5 mm) washed ashore along the USA west coast and virgin plastic pellets over a wavelength range from 350 to 2500 nm. Compared to the spectral variability of multi-colored dry macroplastics, the measured dry marine-harvested microplastic reflectance spectra could be represented as a single bulk average spectrum with notable absorption features at ~931, 1215, 1417 and 1732 nm. The wet marine-harvested microplastics had similar spectral features to the dry microplastics but the magnitude was lower over the measured spectrum. When spectrally matched to the reference library of typical dry virgin pellets, the mean dry marine-harvested microplastics reflectance had moderate similarities to low-density polyethylene, polyethylene terephthalate, polypropylene and polymethyl methacrylate. This composition was consistent with the subset sampled with the Fourier Transform Infrared (FTIR) spectrometer and what has been reported globally. The absorption features at 1215 and 1732 nm were observable through an intervening atmosphere and used to map the distributions of synthetic hydrocarbons at a landfill and on man-made structures from airborne visible-infrared imaging spectrometer (AVIRIS) imagery, indicating the potential to remotely sense dry washed ashore and land-origin plastics. These same absorption features were identifiable on wet marine-harvested microplastics, but the ability to conduct remote sensing of microplastics at the ocean surface layer will require more detailed radiative transfer analysis and development of high signal-to-noise sensors. The spectral measurements presented here provide a foundation for such advances towards remote detection of plastics from various platforms.

1. Introduction

Plastic pollution in the ocean has been identified as a threat for benthic, pelagic and littoral zones (Bergmann et al., 2015; Carpenter et al., 1972; Carpenter and Smith, 1972; Colton et al., 1974; Eerkes-Medrano et al., 2015; GESAMP, 2015; Thevenon et al., 2014; USEPA, 2011). A wide variety of marine organisms can ingest or become entangled in these plastic products with direct and often deadly effects (Carpenter et al., 1972; Cole et al., 2013; Eriksen et al., 2014; Ryan and Moloney, 1993; Thompson et al., 2004). Although large concentrations of floating or suspended plastic debris are being observed or modeled across aquatic habitats from inland to the open ocean, a comprehensive analysis of the spatial extent and abundance of debris is lacking and the monitoring tools are not well developed to assess global distributions (Bergmann et al., 2015; Carpenter and Smith, 1972; Eerkes-Medrano et al., 2015; Eriksen et al., 2014; GESAMP, 2015; Jambeck et al., 2015; Law et al., 2010; Ryan and Moloney, 1993; Thompson et al., 2004; van Sebille et al., 2015). Remote sensing imagery with moderate to high temporal, spectral and spatial resolution would provide an excellent ancillary tool to quantitatively explore the distributions of floating marine plastic debris (Maximenko et al., 2016; Moller et al., 2016).

Interdisciplinary scientific knowledge on plastic debris in the natural environment is required to document the dramatic increase in global uses of plastic over the last half century (Bergmann et al., 2015; SEP, 2011; Wang et al., 2016). Recent publications have outlined several methodological and analytical challenges to assessing marine

* Corresponding author.
E-mail address: shungu.garaba@uconn.edu (S.P. Garaba).

https://doi.org/10.1016/j.rse.2017.11.023
Received 24 April 2017; Received in revised form 9 November 2017; Accepted 21 November 2017
Available online 06 December 2017

plastic size ranges, abundance and polymer types (Eerkes-Medrano et al., 2015; Filella, 2015; Galgani et al., 2013; GESAMP, 2015; Hidalgo-Ruz et al., 2012; Lenz et al., 2015; SEP, 2011; Thevenon et al., 2014; Wang et al., 2016). Despite this, researchers have proposed provisional working terms, sampling and analytical techniques that are used in this investigation. Macroplastics include all particles > 5 mm in diameter and microplastics range from 0.33 to 5 mm in diameter (GESAMP, 2015; Thevenon et al., 2014; USEPA, 2011). The primary sampling method at sea involves deploying neuston nets with a mesh size of ~0.33 mm in the surface layers from a research vessel (Carpenter and Smith, 1972; Law et al., 2010; Masura et al., 2015; Reisser et al., 2013). Harvested plastics are identified and sorted by visual inspection also using a microscope. Polymer composition and type of individual microplastic particles is obtained typically from density separation with subsequent C:H:N analysis, pyrolysis-gas chromatography and Fourier Transform Infrared or Raman spectroscopy (Bergmann et al., 2015; Hidalgo-Ruz et al., 2012; Thevenon et al., 2014).

However, there is a need for integrative direct and indirect monitoring approaches such as remote sensing (Mace, 2012; Maximenko et al., 2016; Slonecker et al., 2010). Remote sensing potentially provides the necessary spatial and temporal coverage of the ocean surface for estimating the global abundance of near sea surface plastics. However, enhanced reflectance due to marine plastics in ocean color imagery may not be observable due to standard processing techniques that remove portions of the signal influenced by atmospheric and sea surface perturbations (Bailey et al., 2010; Gordon and Wang, 1994). Additionally, limited sea-truth information on naturally harvested plastics has constrained the development of quantitative algorithms to remotely detect marine plastics. Therefore, a better understanding of the optical properties of marine plastics and their contributions to the visible and infrared wavelengths is important to assess how these features can be detected and quantified with current and future remote sensing tools.

Plastics have unique inherent optical characteristics in the near infrared (NIR) to shortwave infrared (SWIR) spectrum that have been used in automated optical sorting of waste in the recycling industry (Huth-Fehre et al., 1995; Masoumi et al., 2012; Moroni et al., 2015; Wienke et al., 1995). While reflectance in the visible to near infrared spectrum 400 to 900 nm has been measured on select pieces of macroplastic garbage (Hu et al., 2015), we are not aware of any studies characterizing the spectral properties of marine-harvested macro- and microplastics from the visible to SWIR wavelengths. However, there is a rising interest in the potential applications of remote sensing in detecting hydrocarbons such as oil, plastics and methane utilizing the absorption features in the ultra-violet to longwave infrared spectrum (Asadzadeh and de Souza Filho, 2017; Maximenko et al., 2016; Scafutto et al., 2017).

In this study, we aim to broaden the available information on the spectral properties of macro- and microplastics by conducting analysis on debris harvested from the North Atlantic Ocean and coastal ecosystems along the USA west coast as well as virgin pellets. We investigate the spectral bands and resolution specific to dry and wet marine-harvested plastics. Furthermore, we explore the potential for remote sensing algorithms of plastics using identified inherent plastic absorption bands. The results from this work have applications to sensor design and technology, as well as providing a foundation for more intensive radiative transfer modeling of plastics and experiments in marine ecosystems.

2. Methods and materials

2.1. Reflectance sampling

Spectral reflectance of dry marine-harvested macroplastics was measured outdoors at the Mystic Aquarium in Connecticut, USA on 25 March 2015 around midday (Fig. 1). These macroplastics were collected by the Washed Ashore team of volunteers along the beaches in Oregon and other areas on the west coastline of the USA. No further laboratory analyses were completed on the dry samples because they are part of an ongoing plastic pollution awareness art exhibition called Washed Ashore: Art to Save the Sea.

These specimens represent a wide range of harvested macroplastic debris that have undergone environmental weathering, but do not necessarily represent the most frequently found macroplastic debris on the beaches. Therefore, the spectra should be considered as representative of what might be found, but cannot be statistically aggregated into an “average” bulk signal or type of plastic. Identifiable items included buoys, handles, bottle caps, containers, styrofoam, ropes, toys, diving fins and nets. Item colors included yellow, green, peach, orange, dark brown, beige, light blue, clear, white, glossy white and pale green.

Reflectance measurements were also conducted on microplastics harvested by Sea Education Association team from the top 0.25 m of western North Atlantic waters with a neuston net mesh size of 335 μm (Law et al., 2010). These samples were dried, separated by hand and stored in glass scintillation vials. Samples were further separated by size using successive filters from large to small metal sieves with mesh sizes: 1.68–2.00 mm, 2.00–2.38 mm, 2.38–2.83 mm, 2.83–3.36 mm, 3.36–4.00 mm (Fig. 2). Additional information on refractive indices of known virgin pellets as well as size, color and roundness of these specimens is presented (Supplementary Material Tables S1 and S2). Samples smaller than 1.68 mm were not included because the quantity was not sufficient to obtain a reasonable spectral signal or an optically dense target. Another set of microplastic samples from Kamilo Point, Hawaii, USA was prepared as above but was not of sufficient quantity to separate into size classes and was identified only as particles < 5 mm.

Eleven types of dry virgin pellets were also measured to establish a spectral reference library: polyvinyl chloride (PVC), polyamide or nylon (PA 6.6 and PA 6), low-density polyethylene (LDPE), polyethylene terephthalate (PET), polypropylene (PP), polystyrene (PS), fluorinated ethylene propylene teflon (FEP), terpolymer lustran 752 (ABS), Merlon, polymethyl methacrylate (PMMA). The dry virgin pellets were not colored but had varying opacity (Supplementary Material Fig. S1). Selection of the dry virgin pellets was based on polymer type analysis from prior extensive investigations on sediment and marine-harvested plastic debris (Andrady, 2011; GESAMP, 2015; Hidalgo-Ruz et al., 2012).

A PANalytical Boulder ASD FieldSpec 4 spectroradiometer with a wavelength range from 350 to 2500 nm interpolated to a 1 nm resolution was utilized to measure spectral reflectance of the samples under ambient sunlight during clear sky conditions. Dry microplastics and the virgin pellets were aggregated into an optically dense target on a black rubber mat for a bulk spectral measurement of the sample (Fig. 2). The black rubber used as background material had negligible reflectance. A 1° fore optic pointed vertically downwards was outfitted on the spectrometer at 8 cm above the microplastics along with a 75% Labsphere white Spectralon plaque. For the dry macroplastics, an 8.5° fore optic was pointed at a nadir angle of 45° to the sample at a distance of 10 cm with a 99% white Spectralon plaque. Effects of instrument and user shading on measurements were minimal at this geometry and distance. A measurement was taken over Spectralon followed by 5 (macroplastic) or 10 (microplastic) measurements over the sample and finally another measurement over Spectralon. For the macroplastics, spectra were recorded from five different spots on the stationary art sample. For the microplastics, the sample was gently mixed to rearrange the location and orientation of the particles for each of the 10 replicate bulk measurements. The spectral reflectance of wet microplastics floating on filtered seawater with salinity 30 ppt was also collected following the same methods as above (Supplementary Material Fig. S2). Lambertian-equivalent reflectance (R) was then calculated as the spectrum of the sample normalized to the spectrum obtained over the Lambertian Spectralon plaque. A representative R was determined

Fig. 1. Images of naturally harvested dry macroplastic debris sampled in this study that were part of a public exhibition "Washed Ashore: Art to Save the Sea" at the Mystic Aquarium, Mystic CT, USA.

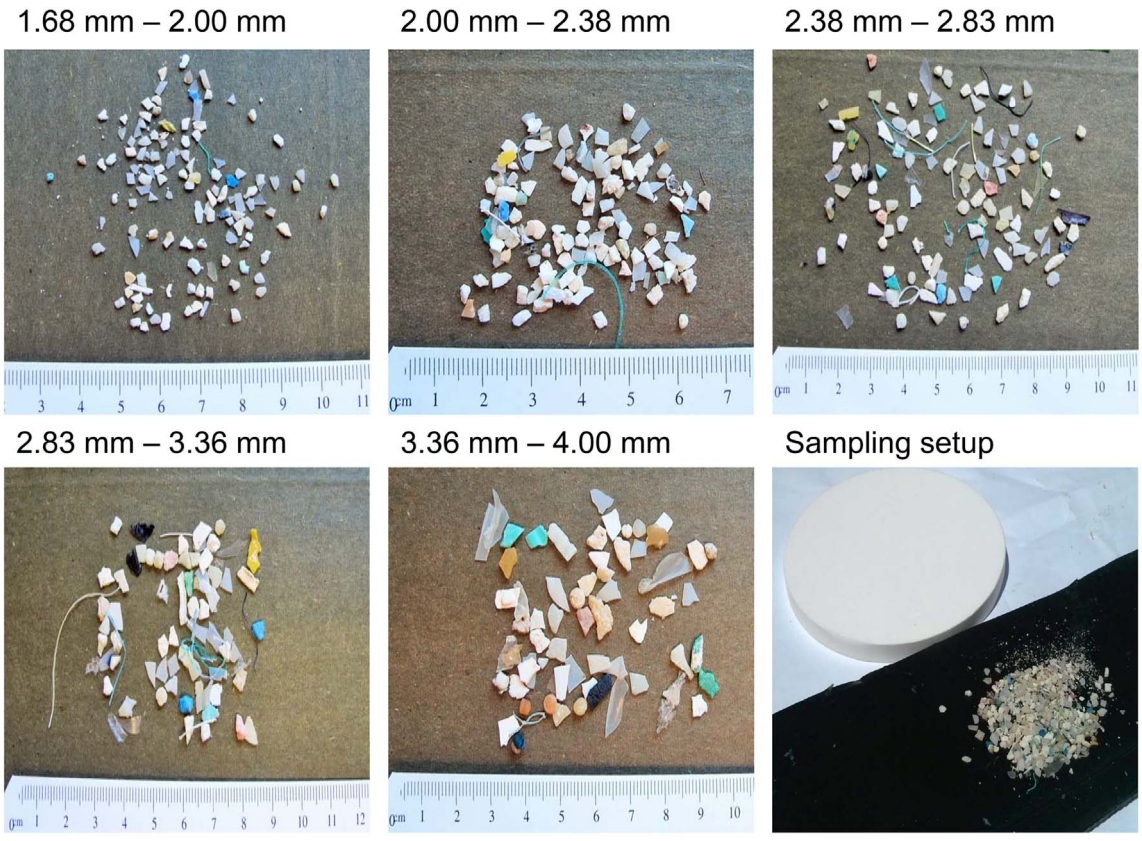

Fig. 2. Images of sampled dry microplastic debris from the North Atlantic Ocean separated into different size classes. The sampling setup in bottom right panel shows a Lambertian Spectralon panel and the aggregated particles on a black rubber background used to obtain a bulk reflectance measurement.

by taking the average of the repetitive measurements of each sample.

2.2. Spectral absorption features and detection indexes

Visual inspection aided in identifying known plastic as well as other salient absorption features, this inspection was further validated by derivative analysis of calculated R. Spectra was smoothed using a moving average filter with a span of 19 nm before derivative analysis. Spectrum derivative analysis is a common technique that has been used to identify absorption features in floating algae, corals and other optically active constituents of natural waters (Dierssen et al., 2015a; Huguenin and Jones, 1986; Russell et al., 2016; Tsai and Philpot, 1998). A relative band depth index algorithm calculated from a linear baseline or continuum line quantified major absorption features (Fig. 3). End- and start point wavebands of the continuum line were determined using a MathWorks MATLAB R2016a convhull function to systematically select the convex hull, the wavelengths immediately preceding and following the absorption waveband. A baseline subtraction approach has been proven to be robust in both determining the presence and inferring the abundance of target optically active constituents in nature (Clark, 1983; Clark, 1999).

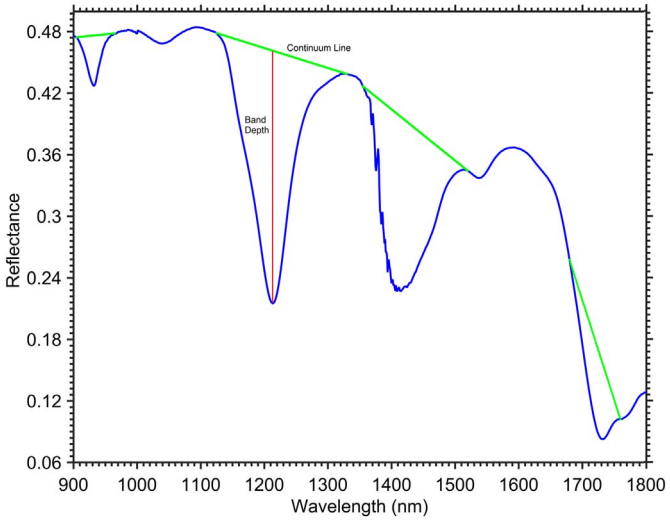

Fig. 3. An example showing the infrared spectral reflectance of a dry marine harvested microplastic sample with continuum lines and band depth highlighted.

2.3. Spectra similarity

Similarity between measured and reference R can be determined using various scoring algorithms (Samokhin et al., 2015). These algorithms provide a form of probability matching. We used the robust spectral contrast angle approach to compute a quantitative spectral similarity score (Wan et al., 2002). Spectral contrast angle approach is an objective similarity analysis of spectra that augments visual analysis. It transforms R into a multi-dimensional vector that is independent of magnitude, which might be a product of environmental perturbations or instrument sensitivity. The spectral contrast angle (Θ) was computed as,

$$\theta = \cos^{-1} \frac{\sum x \cdot y}{\sqrt{\sum x^2 \sum y^2}} \quad (1)$$

where x and y are the individual wavebands of a target reference spectrum and unknown spectrum.

Deciding on the degree of similarity or distinguishing similarity also known as thresholding is challenging and therefore depends on user needs when matching measured spectra to reference libraries (Schwarz and Staenz, 2001; Shanmugam and SrinivasaPerumal, 2014). A $\Theta = 0^\circ$ indicates a high level of spectral shape similarity and $\Theta = 90^\circ$ means lack of spectral identity. Example threshold values that have been used in earlier works include $\Theta = 17.2^\circ$ for a land use mapping study (Petropoulos et al., 2013) and $\Theta = 11.5^\circ$ in a coral mapping campaign (Kutser et al., 2006). Therefore, we defined the goodness of spectral similarity in our study as very strong ($0^\circ \leq \Theta \leq 5^\circ$), strong ($5^\circ < \Theta \leq 10^\circ$), moderate ($10^\circ < \Theta \leq 15^\circ$), weak ($15^\circ < \Theta \leq 20^\circ$) and very weak ($20^\circ < \Theta$). Spearman rank correlation test was implemented as a complementary step in determining the level of spectral association with a statistical significant p-value < 0.05. Furthermore, differences in R within the microplastic sub-size groups after sieving (1.68–2.00 mm, 2.00–2.38 mm, 2.38–2.83 mm, 2.83–3.36 mm and 3.36–4.00 mm) were explored using Kruskal-Wallis one-way analysis of variance. These statistical computations were performed in MathWorks MATLAB R2016a.

2.4. Fourier Transform Infrared spectroscopy analysis

Polymer type analysis of a few individual microplastics particles was completed using a Spectra tech IR Plan Infrared Microscope with a Nicolet Magna 560 Fourier Transform Infrared (FTIR) spectrometer. Each measured spectrum from the FTIR was matched to spectra in the Bio-Rad KnowItAll ATR/IR ID Expert spectral reference library using a first derivative criterion. Polymer types obtained from testing individual particles were used to verify spectral matching analysis between measured bulk spectrum and the new spectral reference library.

2.5. Airborne imagery analysis

Airborne visible-infrared imaging spectrometer (AVIRIS) imagery was retrieved from the AVIRIS online data portal at the National Aeronautics and Space Administration Jet Propulsion Laboratory, USA. The main area of interest was the California Sunshine Canyon Landfill in USA with predominantly plastic waste and surrounding man-made structures. Orthocorrected, calibrated and atmospherically uncorrected radiance information evaluated was from the image (file ID: f111115t01p00r08rdn_c) captured with a pixel size of 7.1 m on 15 November 2011 (Flight Log: f111115t01). Image analysis was performed in SeaDAS version 7.3.2. Band depth was calculated using the at-sensor radiance (L). The 1732 nm feature was applied in the hydrocarbon index (HI_{1732}) algorithm (Kühn et al., 2004) using L at ~1702, 1732 and 1742 nm

$$HI_{1732} = L_{1705nm} - L_{1729nm} + 0.667 \times (L_{1741nm} - L_{1705nm}) \quad (2)$$

The wavebands proposed for HI_{1732} are 1705, 1729 and 1741 nm but were adapted here to the nearest bands available from AVIRIS imagery. For brevity, the AVIRIS waveband values were rounded off in Eq. (2).

2.6. Spectral mixing

Spectral mixture modeling is useful in estimating pixel abundance of unique optically active components in a pixel. The main assumption is that in a given pixel there are optically active components that contribute uniquely to the bulk spectral signal reaching a sensor (Adams et al., 1986; Clark, 1999; Settle and Drake, 1993). The approach provides an approximation assuming that the optically active constituents behave in a linear manner. For the purpose of this study, a simplified linear mixing simulation was completed to model how measured spectral properties of the dry and wet marine-harvested microplastics were influenced by varying pixel coverage with a typical open ocean water-leaving reflectance spectrum measured in the North Atlantic on 13 August 2015 (39.78° North, 71.45° West). We also assume minimal spectral noise ($\Delta R_{noise} \approx 0$) which is dependent on type of optical sensor (Moses et al., 2012). The mixed R_{mix} was calculated as

$$R_{mix} = f_{plastic} \times R_{plastic} + f_{seawater} \times R_{seawater} + \Delta R_{noise} \quad (3)$$

where f is the percentage pixel coverage of each endmember ranging from 0 to 100% to the resulting simulated pixel R_{mix}.

3. Results

3.1. Optical characterization

Measured R from the dry washed ashore macroplastics was highly variable in both magnitude and shape (Fig. 4). As expected, the peaks in the visible spectrum coincided with the apparent color of the object. For example, blue objects peaked in blue wavelengths (400–500 nm) and green objects peaked in green wavelengths (500–550 nm). White objects tended to have a sloping to a nearly flat spectral signal. In addition to spectral shape, the magnitude of the reflectance was also highly variable. Percentage R at 555 nm, for example, varied from $< 5\%$ for the dark blue and orange samples to 70–80% for the white and ivory samples. At 800 nm, R varied from 20% for the dark blue sample to 87% for the beige samples. In the NIR to SWIR wavelengths (~900–2500 nm), there was an overall decrease in R punctuated by several localized dips. Specifically, common spectral features were evident across most of the samples from 905 to 955 nm, 1160 to 1260 nm, 1380 to 1480 nm and 1715 to 1750 nm (part of the shaded regions in Fig. 4). Other absorption features of these macroplastics in the NIR to SWIR were presumably a result of the inherent polymer types of the individual object (Fig. 4).

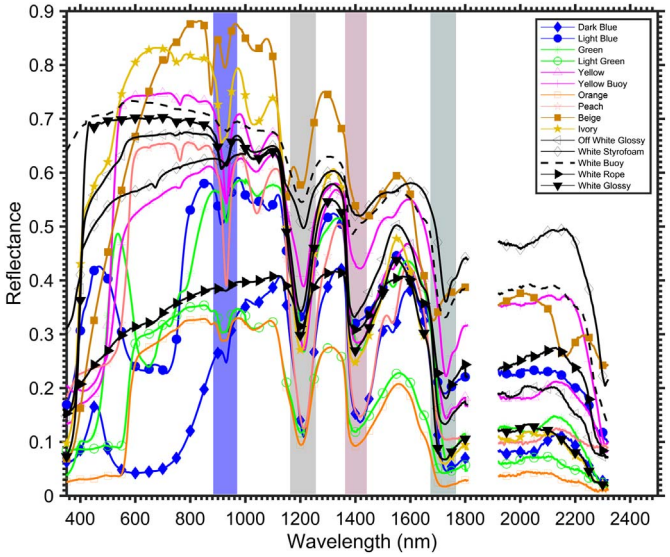

Fig. 4. Reflectance of macroplastics harvested from beaches along the west coast of the USA reveals several spectral dips or absorption features in NIR and SWIR wavelengths (shaded) that are fairly consistent across the variety of plastic objects.

Our analysis of the dry marine-harvested microplastics revealed a relatively consistent R in both spectral shape and magnitude than the macroplastics due to the mixing of the aggregated pieces within the field of view of our spectroradiometer fore optic (Fig. 5A). R was consistent with absorption dips in infrared wavelengths (> 850 nm) that were highly conserved. Percentage ranges over the whole spectrum were $< 40\%$. In the visible, R increased monotonically from ultraviolet to red wavelengths. Highest reflectance was recognized in between 850 and 900 nm.

Kruskal-Wallis analysis showed that there were statistically significant differences ($p < 0.05$) in R over the measured spectrum 350 to 2500 nm within the investigated size groups: 1.68–2.00 mm, 2.00–2.38 mm, 2.38–2.83 mm, 2.83–3.36 mm and 3.36–4.00 mm (Fig. 5B). These differences existed at varying wavebands. More analysis was done by applying Eq. (1) to compare the similarity of the spectra in terms of the spectral shape instead of magnitudes as indicated by the Kruskal-Wallis analysis. Dry marine-harvested microplastics had on average very strong (mean $\Theta < 5^\circ$) spectral shape similarities (Table 1) therefore, a single microplastic R was determined by taking the arithmetic mean of all the measured spectra (Fig. 5C). These microplastics had nearly identical spectral shapes as well as uniform signature plastic absorption features in NIR and SWIR wavelengths i.e. 905 to 955 nm, 1160 to 1260 nm, 1380 to 1480 nm and 1715 to 1750 nm (shaded regions in Fig. 5). Minor absorption features were noted in wavelength ranges of 1030 to 1070 nm, 1510 to 1550 nm, 2000 to 2050 nm and 2300 to 2350 nm (red dotted vertical lines in Fig. 5C). These major and minor absorption features were further confirmed using derivative analysis (Fig. 5D).

The spectral reflectance of wet marine-harvested microplastics was measured to simulate the potential sensing of wet microplastics floating on the sea surface (Fig. 6). Reflectance of wet particles decreased on average by 56 ± 23% compared to dry particles with a spectral dependence increasing with wavelength from 12% in the UV to nearly 90% in the SWIR.

3.2. Spectral similarity of macro- and microplastics

Spectra similarity measures were derived from Eq. (1) and the findings for both the macro- and microplastics results are summarized below (Table 1). The similarity analysis was targeted at the major absorption wavebands i.e. 905 to 955 nm, 1160 to 1260 nm, 1380 to 1480 nm and 1715 to 1750 nm. The goal was to assess the similarity between the R spectra from our macro- and microplastic samples. Further analysis of similarity over the whole wavelength range 350 to 2500 nm was aimed at evaluating the spectral homogeneity of the macroplastics, in particular differences due to their inherent color in the visible wavelength range and polymer types. Spearman rank correlation tests did not provide a completely objective way to deduce spectral similarity, but confirmed statistically significant ($p < 0.05$) strong to very strong positive monotonic relationships among these measured spectra.

The spectral contrast angle investigation suggested that each macroplastics sample was different from the others when assessed over the whole measured spectrum (350–2500 nm) with weak spectral similarities Θ averaging 19.1°. In comparison, the microplastic R spectra were closely identical over the whole measured spectrum (350–2500 nm) with very strong spectral similarities Θ averaging 4.6°. In general, at the major absorption features for both macro- and microplastics (i.e. 905 to 955 nm, 1160 to 1260 nm, 1380 to 1480 nm and 1715 to 1750 nm) we obtained strong to very strong spectral similarities with an average Θ of $< 8^\circ$.

3.3. Spectral classification of plastic composition

We measured R for eleven individual samples of dry virgin pellets (Fig. 7). The dataset is available on the online repository of Ecological Spectral Information System (Garaba and Dierssen, 2017). Visual inspection and spectral similarity investigations showed that these polymers had different R spectral properties from each other. Percentage range differences in R varied from 50 to 80% over the whole measured wavelength 350 to 2500 nm. PVC had the highest peak reflectance reaching 96% in the green to infrared spectrum, 550 to 1150 nm and PET had the lowest for the same wavelength range. With the exception of FEP, most of the spectra had lower R in ultraviolet wavelengths that increased sharply into blue wavelengths. Most of the dry virgin pellets were spectrally flat throughout most of the visible to NIR wavelengths. Inherent absorption features were prominent in the NIR to SWIR wavelength ranges > 850 nm.

Similarity analysis suggested that all of the virgin pellets were spectrally heterogeneous with the exception of PA 6.6 and PA 6. These two forms of nylon samples had a very strong spectral similarity

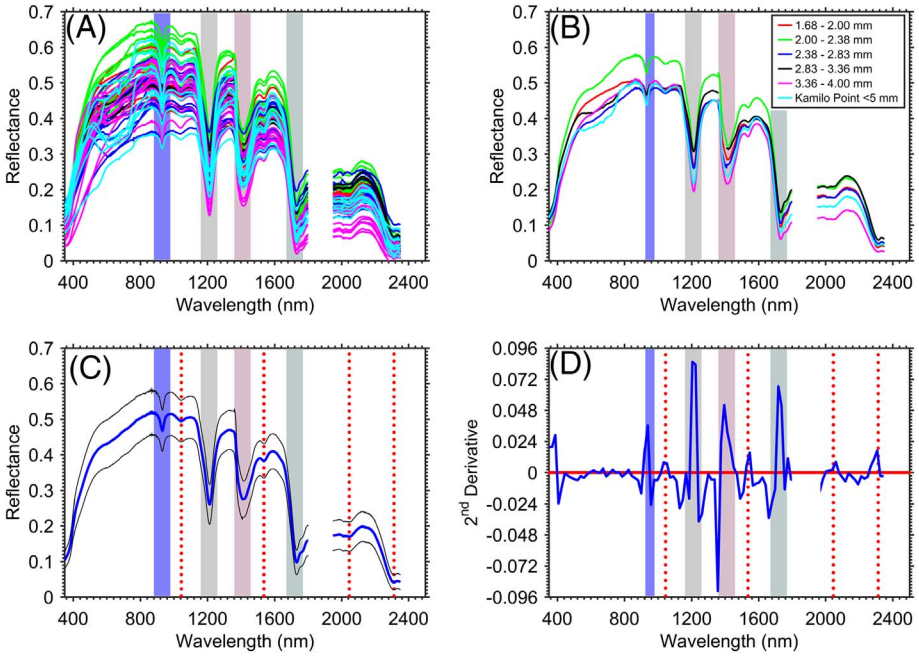

Fig. 5. (A) Bulk reflectance spectra of aggregated dry marine-harvested microplastics colored by size class (legend in panel B). (B) Mean reflectance of each size class. (C) Average reflectance with 1 standard deviation continuous error bars with shaded regions and red dotted lines indicating major and minor absorption features respectively. (D) Second derivative spectra of the mean reflectance spectrum. (For interpretation of the references to color in this figure legend, the reader is referred to the web version of this article.)

Table 1
Descriptive statistics from the spectral contrast angle similarity test for the dry microplastics and macroplastics with respect to each spectra in the corresponding category.

	Θ [°] 905–955 nm	Θ [°] 1160–1260 nm	Θ [°] 1380–1480 nm	Θ [°] 1715–1750 nm	Θ [°] 350–2500 nm
Macroplastics					
Mean ± stdev	2.5 ± 1.9	7.3 ± 3.9	4.5 ± 2.6	3.1 ± 2.3	19.1 ± 7.1
Min, max	0.1, 7.6	0.8, 15.6	0.7, 10.5	0.2, 9.0	5.7, 38.2
Microplastics					
Mean ± stdev	0.6 ± 0.4	2.3 ± 1.9	4.8 ± 1.9	1.6 ± 1.2	4.6 ± 2.6
Min, max	0.03, 2.5	0.02, 12.0	0.32, 14.9	0.05, 10.0	0.1, 16.8

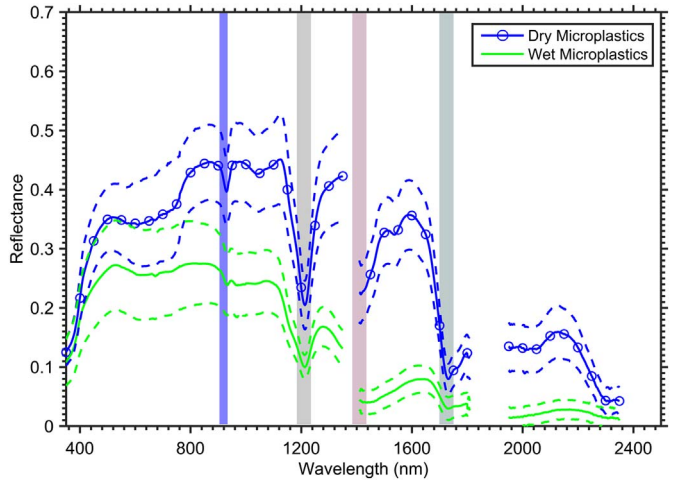

Fig. 6. Average dry and wet marine-harvested microplastics reflectance with 1 standard deviation continuous dashed error bars with shaded regions indicating absorption features. Filtered seawater 30 ppt was used to wet the dry marine-harvested microplastics.

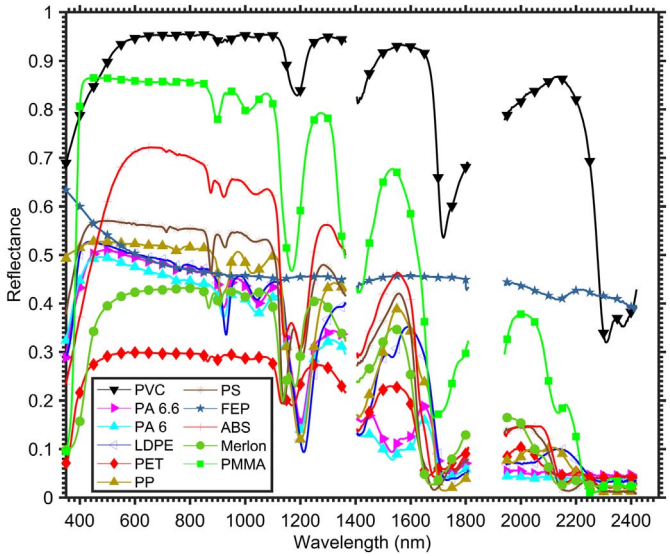

Fig. 7. Reflectance of dry virgin pellets; polyvinyl chloride (PVC), polyamide or nylon (PA 6.6 and PA 6), low-density polyethylene (LDPE), polyethylene terephthalate (PET), polypropylene (PP), polystyrene (PS), fluorinated ethylene propylene teflon (FEP), terpolymer lustran 752 (ABS), Merlon, polymethyl methacrylate (PMMA).

Θ = 2.1° despite having different appearances i.e., PA 6.6 pellets were more clear than PA 6 (Supplementary Material Fig. S1). Endmember spectra of these virgin pellets were compared to the measured R from the dry marine-harvested macro- and microplastics using Eq. (1) over the wavelength range where the unique plastic absorption features were found in the NIR to SWIR wavelengths > 850 nm. Moderate to very strong similarities, Θ less than or equal to 15°, were highlighted (Table 2).

A summary of the spectral similarity analysis (Table 2) indicated that among the dry macroplastic objects many had matches to one or

Table 2
Spectral contrast angle comparison between typical dry virgin pellets and marine-harvested plastics. The values that had a very strong to moderate similarity (Θ ≤ 15°) are highlighted in bold.

Macroplastics	PVC	PA 6.6	PA 6	LDPE	PET	PP	PS	FEP	ABS	Merlon	PMMA
Dark Blue	24.5	26.3	27.0	**13.9**	21.1	**14.3**	20.8	29.5	19.9	22.6	18.4
Light Blue	15.6	21.9	22.7	15.5	**13.8**	**14.1**	15.9	20.3	15.2	16.9	**10.4**
Green	23.7	17.4	18.3	**8.7**	**13.5**	**8.9**	**14.0**	28.6	**12.0**	16.1	**12.3**
Light Green	26.8	**14.6**	15.4	**8.1**	**11.8**	**5.6**	**11.2**	31.4	**8.2**	**13.8**	**12.3**
Yellow	21.5	17.1	17.8	**9.7**	**14.4**	**9.8**	15.4	25.9	**13.2**	17.6	**12.9**
Yellow Buoy	**9.2**	28.1	28.9	20.8	19.4	20.0	21.5	15.1	21.4	22.3	**14.7**
Orange	31.8	**13.0**	**13.5**	**9.0**	**13.7**	**6.5**	**12.0**	36.3	**8.7**	**14.8**	15.8
Peach	28.0	16.0	16.5	**6.2**	18.3	**8.8**	18.0	31.9	**15.0**	20.7	18.0
Beige	15.7	22.7	23.4	19.0	**12.6**	17.1	**14.9**	19.0	15.2	15.7	**10.2**
Ivory	30.0	**12.3**	**13.0**	**8.3**	**13.4**	**6.5**	**12.5**	34.5	**9.1**	15.1	**14.8**
Off White Glossy	20.8	18.5	19.3	**11.2**	**11.4**	**9.5**	**12.6**	25.6	**11.2**	**14.2**	**9.2**
White Styrofoam	**3.7**	33.0	33.7	26.9	23.9	26.0	26.4	**9.0**	26.8	26.8	19.4
White Buoy	**9.6**	27.3	28.0	21.8	17.9	20.7	20.7	**14.5**	20.8	21.0	**13.6**
White Rope	**7.9**	30.7	31.5	23.2	20.4	22.1	22.8	**14.1**	23.2	23.1	15.6
White Glossy Micropalstics	27.2	**13.6**	**14.5**	**8.8**	**11.0**	**6.6**	**10.8**	31.9	**7.9**	**13.1**	**11.8**
Mean	16.6	22.2	23.0	**14.2**	**14.9**	**13.7**	16.7	22.7	15.8	18.0	**11.6**

more polymer types. In particular, there were strong to very strong similarities to PVC and moderate to strong similarities to LDPE, PP, FEP, ABS and PMMA. However, we derived moderate similarities of the macroplastics to PA, PA 6.6, PET, PS and Merlon.

In the microplastics, the average bulk *R* had moderate similarities to PMMA (Θ = 11.6°) followed by PP (Θ = 13.7°), LDPE (Θ = 14.2°) and PET (Θ = 14.9°). Visual inspection of normalized *R* spectra of these raw polymer types and the microplastic bulk mean displayed some resemblances in terms of spectral shape with the absorption features occurring at identical wavebands or slightly shifted (Fig. 8).

A subset of 10 randomly selected microplastic particles were analyzed using FTIR microscopy. The highest probability matches were to PP or PP isotactic (Supplementary Material Fig. S3). Further analysis using Raman spectroscopy of the individual microplastic particles harvested by the Sea Education Association team is still ongoing with current results of 718 pieces from 24 separate tows suggesting 83% PE, 5% PP, < 1% PS, 11% no reading (Donohue et al., 2016).

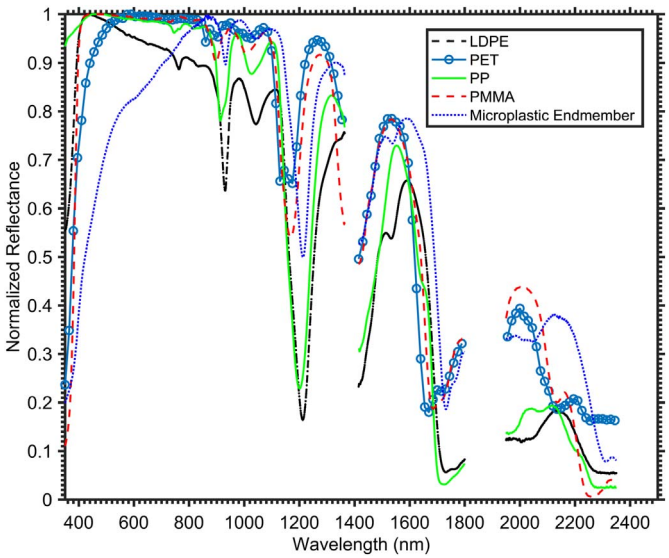

Fig. 8. Normalized reflectance of the marine-harvested microplastics bulk mean, virgin pellets of low-density polyethylene (LDPE), polyethylene terephthalate (PET), polypropylene (PP) and polymethyl methacrylate (PMMA).

3.4. Band depth indexes

Band depth indexes were calculated at the identified absorption features: ~931, 1215, 1417 and 1732 nm for both the macro- and microplastics sampled in this study. The indexes of each group macro- and microplastics fell within the range of the other (Table 3). The largest average band depth was found at 1215 nm and smallest band depth at 931 nm. In the dry and wet microplastics, the signal around the 1417 nm had a low signal-to-noise due to high atmospheric absorption and band depths were not calculated at this waveband.

3.5. Mapping synthetic hydrocarbons using airborne imagery on land

A feasibility assessment was conducted using hyperspectral AVIRIS imagery to remotely sense hydrocarbon bearing materials using the absorption features identified above. Because airborne hyperspectral imagery of marine plastics was not available for this test, we conducted a case study using dry plastic targets on land to simulate the potential for mapping dry washed ashore and land-origin plastics. As identified above, four spectral regions in the NIR to SWIR were considered unique to the marine-harvested microplastics. We first evaluated these wavebands in the context of atmospheric absorption properties. Modeled transmittance spectrum of atmospheric gases (Fig. 9A), revealed that two of the absorption features from the microplastics coincided with absorption bands of water, in particular around 950 and 1400 nm. However, the 1215 and 1732 nm spectral features seemed least likely to be affected by atmospheric gases (Fig. 9A).

These features were further investigated in the at-sensor radiance spectra measured with AVIRIS over a landfill containing plastic waste material and surrounding areas with man-made structures. Example spectra from natural and man-made target materials (Fig. 9B) were selected from the red = 647.97 nm, green = 550.30 nm, blue = 453.07 nm color composite AVIRIS image (Fig. 10A) for pixels covered by vegetation, water, highway roads, plastic bearing targets such as landfill and industrial warehouse rooftop. Spectra from water, was generally low (< 0.1 normalized radiance units) decreasing to zero in the NIR to SWIR, with no major absorption features matching those of the microplastic bulk mean *R* except around 950 nm. Vegetation had a red-edge feature around 680 nm. All other target materials had nearly similar spectral shape except at 1215 and 1732 nm. At these wavebands, the landfill and rooftop spectra had spectral dips consistent with the absorption features identified in our microplastic bulk mean *R*.

We therefore utilized these two bands to test algorithms for automated mapping of plastics or hydrocarbon bearing materials. We developed a new hydrocarbon index (HI_{1215}) algorithm to capture the absorption feature at ~1215 nm:

Table 3
Descriptive statistics on band depth indexes for absorption bands of macro- and microplastics.

	931 nm	1215 nm	1417 nm	1732 nm
Dry macroplastics				
Mean ± stdev	0.05 ± 0.05	0.23 ± 0.10	0.16 ± 0.07	0.06 ± 0.03
Median, min, max	0.03, 0.01, 0.21	0.21, 0.09, 0.43	0.14, 0.06, 0.29	0.06, −0.01. 0.10
Dry microplastics				
Mean ± stdev	0.04 ± 0.01	0.23 ± 0.04	–	0.07 ± 0.01
Median, min, max	0.04, 0.03, 0.06	0.22, 0.17, 0.29	–	0.07, 0.05. 0.09
Wet microplastics				
Mean ± stdev	0.01 ± 0.01	0.09 ± 0.03	–	0.02 ± 0.01
Median, min, max	0.01, 0.002, 0.02	0.10, 0.03, 0.12	–	0.02, 0.01. 0.02

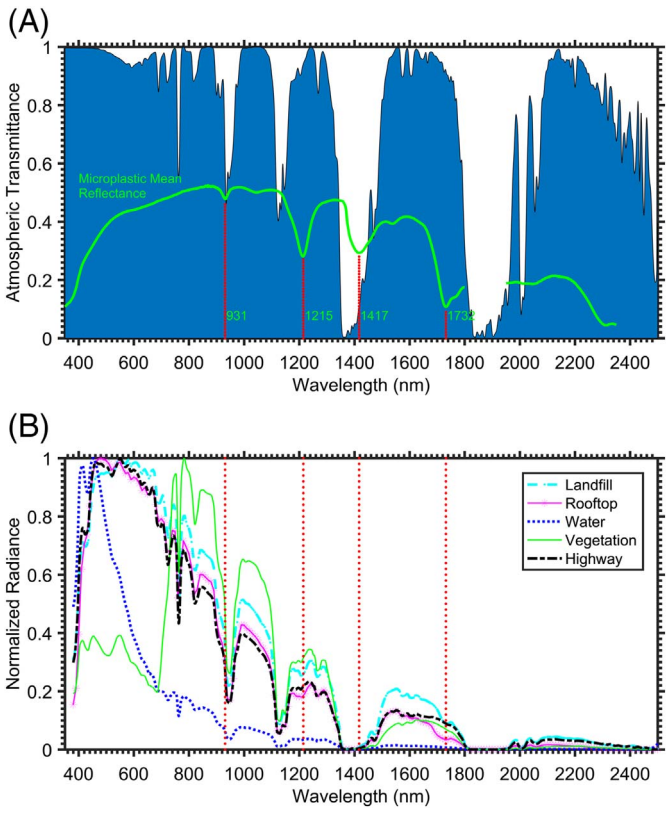

Fig. 9. (A) Modeled atmospheric transmittance spectrum (Gao et al., 2000) showing the spectral regions where the identified features in the dry marine-harvested microplastic bulk mean signal could be observed through an intervening atmosphere. (B) Example normalized radiance of different target pixels (landfill, industrial warehouse rooftop, water, vegetation and highway) in the AVIRIS imagery of the California Sunshine Canyon Landfill, USA.

$$HI_{1215} = L_{1197nm} - L_{1216nm} + 0.5 \times (L_{1235nm} - L_{1197nm}) \quad (4)$$

For brevity, the AVIRIS waveband values were rounded off in Eq. (4). In a prior study, the absorption feature around 1732 nm (Eq. (2)) was proposed and proven to be useful in detecting synthetic hydrocarbons in a remote sensing algorithm (Kühn et al., 2004). Hence, it was appropriate to evaluate it in the mapping of plastics, which are all groups of hydrocarbons. Both HI_{1215} and HI_{1732} maps were noted to highlight several man-made targets with moderate to strong concentrations of hydrocarbons or plastics (Fig. 10B and C). These targets included the Sunshine Canyon landfill, rooftops presumably made of synthetic single-ply material on industrial warehouse in the Sylmar area and a water reservoir at the Metropolitan Water District plant (highlighted in Fig. 10A).

Histogram analysis of representative pixels of vegetation, industrial warehouse rooftop, highway, water and landfill selected by extracting only pixels with dense concentration of target material with the aid of the RGB image verified how these hydrocarbon indexes can be used to potentially map dry hydrocarbon bearing materials (Fig. 10D–F). Furthermore, these mapped indexes agree well with our calculated indexes from the dry microplastic mean R at the 1215 nm absorption feature (0.23 ± 0.05), which was greater than the 1732 nm absorption feature (0.09 ± 0.01) for the microplastics (Table 3). A Spearman rank correlation between HI_{1732} and HI_{1215} (correlation coefficient of 0.7, $p < 0.05$), suggested these two algorithms share a statistically significant positive association as hydrocarbon proxies.

3.6. Spectral mixing

The magnitude of R and absorption features of both dry and wet marine-harvested microplastics were observed to decrease with simulated increase in pixel coverage or bulk spectral contribution by seawater over the spectrum range 350 to 2500 nm (Fig. 11). This decrease in reflectance and absorption feature magnitude was also more pronounced in the wet microplastics compared to the dry microplastics.

Further analysis on the changes in band depth with decreasing abundance was conducted at the two wavebands observable through an intervening atmosphere 1215 and 1732 nm (Table 4). In our simplified simulations, we calculated a three-fold drop at 1215 nm and five-fold at the 1732 nm in the band depth from dry to wet marine-harvested microplastics.

4. Discussion

4.1. Optical characterization of marine-harvested plastics

We present some of the first R spectra from ultraviolet to SWIR (350–2500 nm) of marine plastics harvested from natural marine ecosystems. Nearly all of the dry and wet marine-harvested macro- and microplastics exhibited absorption features centered at 931, 1215, 1417 and 1732 nm. These absorption features especially in the infrared (i.e., ~1200, 1420, 1730, 2310 nm) have been crucial in remote sensing efforts of hydrocarbons such as oil, methane and plastic debris in the natural environment (Asadzadeh and de Souza Filho, 2017; Chung et al., 1999; Cloutis, 1989; Hörig et al., 2001; Huth-Fehre et al., 1995; Kühn et al., 2004; Moroni et al., 2015; Scafutto et al., 2017; Singh, 1995) and are important in automated optical sorting of plastics at garbage recycling centers (Huth-Fehre et al., 1995; Masoumi et al., 2012; Vázquez-Guardado et al., 2015).

Since the sampled macroplastics do not represent a quantitative measure of what is found in nature, we chose not to aggregate or establish an average R from macroplastics and present the variability in spectra that can be found in the natural environment. However, the microplastic samples were collected in a quantitative manner at sea and the average dry marine-harvested microplastic R established here can be treated as a bulk measure of the types of plastics found floating in surface waters of the North Atlantic. The marine-harvested microplastic pieces were remarkably consistent in spectral properties with a general white appearance, similar magnitude and spectral shape across all size

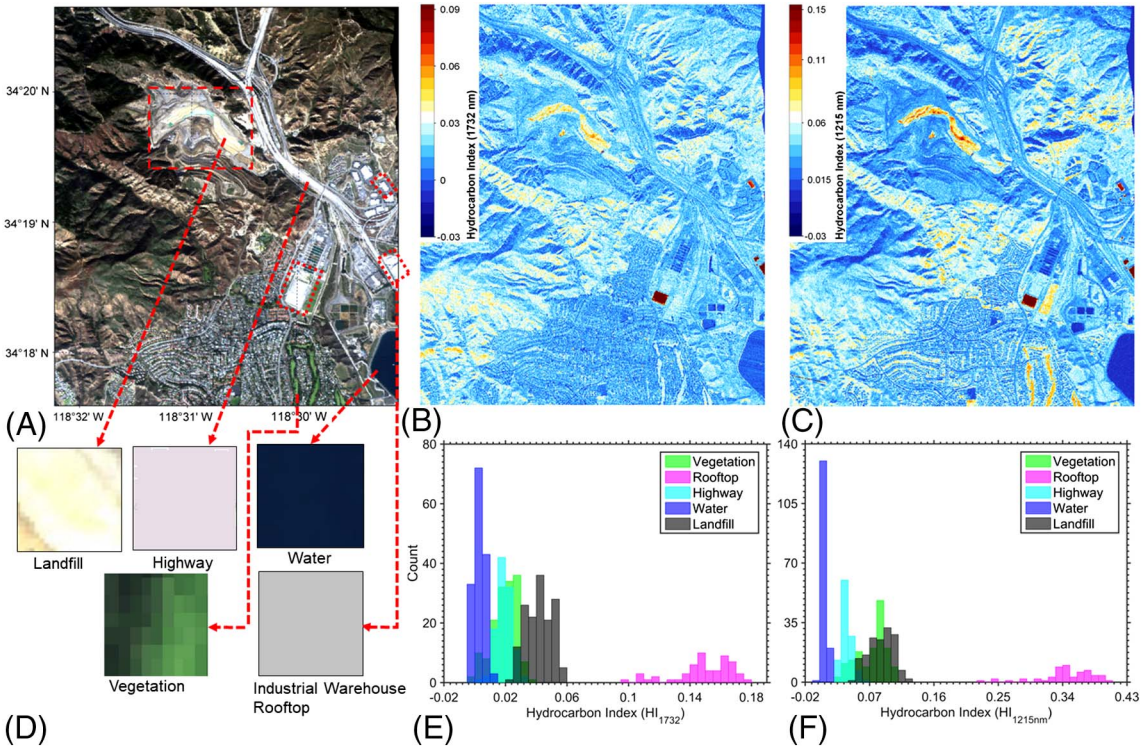

Fig. 10. (A) RGB (Red = 647.97 nm, Green = 550.30 nm, Blue = 453.07 nm) color composite AVIRIS image of the areas near Sunshine Canyon Landfill in California, USA and Metropolitan Water District plant. Highlighted in red dotted boxes are targets showing high concentrations of material with absorption features at 1215 and 1732 nm. (B) Hydrocarbon index (HI_{1732}) map based on absorption feature at 1732 nm. (C) Hydrocarbon index (HI_{1215}) map based on absorption feature at 1215 nm. (D) Target pixels used in the histogram analysis for the (E) HI_{1732} index and (F) HI_{1215} index. (For interpretation of the references to color in this figure legend, the reader is referred to the web version of this article.)

classes. Spectral shape similarity tests between the microplastic bulk mean *R* and the raw polymers produced moderate similarities to PMMA, PP, LDPE and PET. However, this does not necessarily mean each microplastic particle was made of these polymers, but rather the collective bulk signal exhibited similarities to these raw polymers. The best-matched raw polymers (in particular PP, LDPE or PET) identified here were also reported from spectroscopy analyses of individual particles harvested in Atlantic waters (Donohue et al., 2016; Kanhai et al., 2017; Lenz et al., 2015). We also found out that, samples investigated using FTIR were PP or PP isotactic. PP is a widely used polymer in packaging and dishwasher safe containers with a low toxic hazard level. It has a low density (0.895 and 0.92 g/cm^3) which means it has a higher probability of being found floating at the surface of natural waters (Bergmann et al., 2015; Lithner et al., 2011).

Our results suggest that natural samples cannot be perfectly matched to raw polymers because they originate as blended materials that are subject to weathering and degradation in nature. Polymer blends are widely used in everyday plastics and are a combination of different pure polymers present in our spectral reference library, that are typically mixed to improve strength or durability of the plastic end-product (Shah et al., 2008). The resulting optical features of the blended materials will therefore exhibit a combination of spectral characteristics of the additive polymer types. A number of studies have also reported that macroplastics break down into smaller particles slowly in nature and can be subject to considerable weathering at the sea surface. In this long-term process, these macroplastics may be

Table 4
Hydrocarbon indexes for the simulated linear mixing performed with reflectance of North Atlantic seawater, dry and wet marine-harvested microplastic to estimate R_{mix} in Eq. (3).

R_{mix} =	HI_{1215}		HI_{1732}	
	Dry	Wet	Dry	Wet
$0.25*R_{plastic} + 0.75*R_{seawater}$	0.015	0.005	0.011	0.002
$0.5*R_{plastic} + 0.5*R_{seawater}$	0.030	0.010	0.022	0.004
$0.75*R_{plastic} + 0.25*R_{seawater}$	0.044	0.015	0.033	0.006
$1*R_{plastic} + 0*R_{seawater}$	0.059	0.020	0.044	0.008

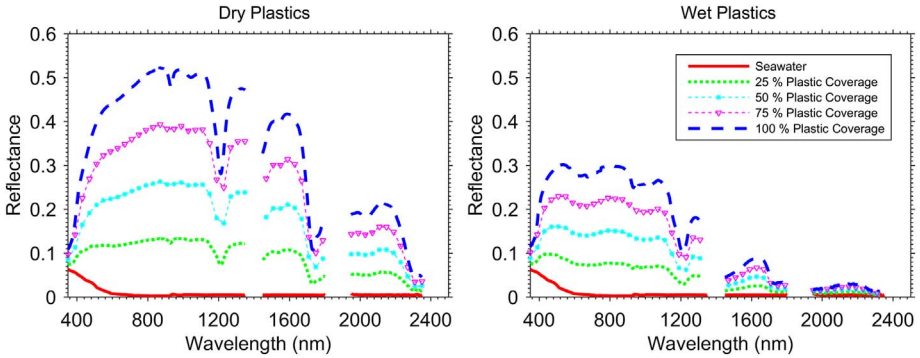

Fig. 11. Spectral mixing simulations using North Atlantic seawater and marine-harvested microplastics (dry and wet) endmembers.

discolored, degraded by photo-oxidation UV exposure and fragmented into microplastics (GESAMP, 2015; Shah et al., 2008; Shaw and Day, 1994; Thevenon et al., 2014). Natural weathering has been identified as a process that alters chemical and physical properties in synthetic polymers. This could be related to how the spectral properties of the bulk microplastics are more uniform in comparison to those of macroplastics, especially with respect to loss of color and carbon-oxygen bond breakages (Kaynak and Sarı, 2016; Zaidi et al., 2010).

Determining the age or residence time of plastic debris collected at sea is still a challenge (Bergmann et al., 2015; Thevenon et al., 2014). However, given the breakdown processes, one might presume that the smaller pieces of microplastics are older than the larger ones and may be more bleached in color. However, we did not see any clear trend in the reflectance for the different size classes studied here. Hence, more research is warranted in terms of understanding the time scales of bleaching, residence times at the sea surface and rates of breakdown into microplastics. These aspects may also reveal additional information about changes in optical properties and chemical composition as the plastic ages in the ocean (Ivar do Sul and Costa, 2014; Shah et al., 2008; Thevenon et al., 2014).

The microplastics studied here were devoid of obvious surfactants due to collection process. Surfactants may change the physiochemical composition and spectral properties of the plastics with time as they adsorb, react and accumulate biofouling organisms, toxics or other pollutant loads (Bergmann et al., 2015; SEP, 2011; Thevenon et al., 2014). Spectral properties and density linked to particle buoyancy can change due to biofouling (Bergmann et al., 2015; Fazey and Ryan, 2016). Biofouling was not considered in this study and requires additional analyses to assess its impact on the spectral properties, the buoyancy and potential for remote sensing.

This study was focused on spectral properties of marine-harvested microplastics, but increasing attention is being placed on nanoplastics in the size range < 100 nm (Andrady, 2011; Koelmans et al., 2015; Ward and Kach, 2009). It remains to be seen whether there would be a correlation between surface concentrations of microplastics and nanoplastics. Nanoplastics may not be as buoyant, may not be dispersed at the sea surface like microplastics and may be more challenging to investigate with remote sensing techniques.

4.2. Outlook for remote sensing from suborbital and satellite missions

Airborne imagery of marine plastics was not available to us, but we demonstrate the potential for remote sensing using high spatial (7.1 m) and spectral resolution (224 bands) AVIRIS imagery of plastic bearing material around a landfill and in neighboring industrial and water treatment facilities. We used at-sensor radiance information to mitigate potential errors that might arise from atmospheric correction algorithms consequently masking absorption features related to plastics. We also highlight the potential of using absorption features at 1215 and 1732 nm with an intervening atmosphere.

The HI_{1215} and HI_{1732} algorithms were able to highlight mostly hydrocarbon or plastic pixels on the white wastewater treatment reservoir and the industrial roofing materials (Fig. 10). However, we observed an overlap (histogram analysis in Fig. 10F) between vegetated pixels and mixed hydrocarbon bearing pixels on the landfill, particularly from the HI_{1215} algorithm. Vegetation consists of many natural hydrocarbons or polymers, namely cellulose, starch and lignin (Verdebout et al., 1995), that have some similar absorption features to synthetic hydrocarbons like plastics. Vegetated pixels could be differentiated from plastics in a stepwise approach using a normalized vegetation difference index (Rouse et al., 1973) or floating algae index for oceanic observations (Hu et al., 2015). Overall, our results suggest that both algorithms are able to identify pixels concentrated with plastics, but the HI_{1732} algorithm is more sensitive to lower concentrations of plastics and has fewer false positives compared to the HI_{1215} algorithm.

With the exception of whitecaps, bubbles, floating vegetation debris (e.g. pieces of wood, leaves, seagrass wrack) as well as very high suspended sediments (Dierssen et al., 2015b; Hu et al., 2015; Knaeps et al., 2015), open ocean reflectance is generally negligible in the NIR to SWIR wavelengths (Kou et al., 1993; Röttgers et al., 2014). Enhancements in reflectance due to floating ocean plastics might be evident in the NIR to SWIR wavelengths allowing detection of ocean plastics. However, the ability to detect different absorption features will depend on the concentration of plastic particles, whether they are dry or wet, and the degree of submergence in the water column, as well as the configuration of the specific sensor designed for this application. Additional sensitivity analyses would be warranted to evaluate how different atmospheric correction routines can be improved such that these features are not removed as part of a whitecap or aerosol correction (Bailey et al., 2010; Gordon and Wang, 1994).

In the natural world, plastic particles, although buoyant, may not be restricted to the sea surface and can be submerged. The concentrations of microplastic particles have been estimated to decrease exponentially with depth (Kooi et al., 2016; Reisser et al., 2015). The results of our study, including the spectral and size information, can be coupled with radiative transfer modeling and coupled atmospheric-ocean models to determine the potential and limitations for detecting marine plastics using various remote sensing techniques.

Although the samples were not perfectly matched to any virgin pellets, there could be value in comparing remotely sensed spectra with features found in the virgin pellets spectral reference library to further diagnose the types of plastics found in different regions of the world. There would obviously be limitations in conducting such an analysis with atmospheric correction and accounting for dilute concentrations of plastics within a pixel. However, we note that spectral measurements offer a non-invasive, quick and effective method to assess particles and could be used as part of the field validation effort to assess marine debris from different parts of the world ocean. The development of optical remote sensing techniques could lead to better assessments of the extent and persistence of plastics in the environment and essentially more informed management of plastic debris pollution.

Remote sensing of plastic debris from a distance is still in the early phases, but some initial investigations have successfully detected marine litter, marine plastics and terrestrial borne plastic products using different optical sensors (Aoyama, 2016; Driedger et al., 2013; Hasituya et al., 2016; Hörig et al., 2001; Kühn et al., 2004; Novelli and Tarantino, 2015; Pichel et al., 2012; Slonecker et al., 2010). Our results suggest that sensors with the appropriate spectral and spatial resolution could potentially provide a resource to assess the location and extent of aggregations of hydrocarbons like plastics in the natural environment. In addition, remote sensing tools could be included as part of integrated multi-disciplinary strategy to quantify plastic debris in the natural environment which includes ship and mooring measurements and models.

Indeed, the apparent spatial, temporal and spectral resolutions of the operational spaceborne ocean color sensors have limited the application of such observations of processes in boundary habitats, such as frontal zones where surface debris tends to aggregate. At present, there is a gap in our observational capabilities from space where no strategy provides the combination of simultaneous medium to high spatial, spectral as well as temporal resolution observations and at the required radiometric quality to assess the distributions of such boundary habitats where plastic particles may aggregate. A combination of spaceborne polar and geostationary observations, suborbital systems, field campaigns and models needs to be developed over the next decade to push forward our understanding of processes occurring along boundary habitats. Our analysis of AVIRIS imagery and the dry marine-harvested samples highlights the possibility of detecting dry washed ashore and land-origin plastics. Additionally, the assessment of the wet marine-harvested plastics indicated the potential of remote sensing of floating plastics. Therefore, the spectral measurements presented here provide a much-needed foundation for the development of technology and algorithms for remote sensing of marine plastics from a variety of platforms.

Acknowledgments

We thank Institute of Materials Science at University of Connecticut, Mystic Aquarium, Anna-Marie Cook and Bill Robberson at the US EPA Region 9 Marine Debris Program, Kara L. Law, Jessica Donohue and the Sea Education Association for the microplastics samples. Funding was provided by NASA Ocean Biology and Biogeochemistry Grant No. NNX15AC32G. We appreciate the support from Brandon J. Russell, Adam Chlus and Kaylan Randolph who assisted with sampling. We thank NASA JPL for providing open access to AVIRIS imagery. Constructive feedback from Gregory Asner, Tiit Kutser, Chuanmin Hu and anonymous reviewers helped improve the manuscript.

Appendix A. Supplementary data

Supplementary data to this article can be found online at https://doi.org/10.1016/j.rse.2017.11.023.

References

Adams, J.B., Smith, M.O., Johnson, P.E., 1986. Spectral mixture modeling: a new analysis of rock and soil types at the Viking Lander 1 Site. J. Geophys. Res. Solid Earth 91, 8098–8112. http://dx.doi.org/10.1029/JB091iB08p08098.

Andrady, A.L., 2011. Microplastics in the marine environment. Mar. Pollut. Bull. 62, 1596–1605. http://dx.doi.org/10.1016/j.marpolbul.2011.05.030.

Aoyama, T., 2016. Extraction of marine debris in the Sea of Japan using high-spatial-resolution satellite images. In: Frouin, R.J., Shenoi, S.C., Rao, K.H. (Eds.), Proceedings of SPIE, Remote Sensing of the Oceans and Inland Waters: Techniques, Applications, and Challenges. 9878. pp. 7. http://dx.doi.org/10.1117/12.2220370. (New Delhi, India).

Asadzadeh, S., de Souza Filho, C.R., 2017. Spectral remote sensing for onshore seepage characterization: a critical overview. Earth Sci. Rev. 168, 48–72. http://dx.doi.org/10.1016/j.earscirev.2017.03.004.

Bailey, S.W., Franz, B.A., Werdell, P.J., 2010. Estimation of near-infrared water-leaving reflectance for satellite ocean color data processing. Opt. Express 18, 7521–7527. http://dx.doi.org/10.1364/OE.18.007521.

Bergmann, M., Gutow, L., Klages, M. (Eds.), 2015. Marine Anthropogenic Litter. Eprint ID 37207 of the Alfred-Wegener-Institut Helmholtz-Zentrum für Polar- und Meeresforschung. Springer International Publishing.

Carpenter, E.J., Smith, K.L., 1972. Plastics on the Sargasso sea surface. Science 175, 1240–1241. http://dx.doi.org/10.1126/science.175.4027.1240.

Carpenter, E.J., Anderson, S.J., Harvey, G.R., Miklas, H.P., Peck, B.B., 1972. Polystyrene spherules in coastal waters. Science 178, 749–750. http://dx.doi.org/10.1126/science.178.4062.749.

Chung, H., Choi, H.J., Ku, M.S., 1999. Rapid identification of petroleum products by near-infrared spectroscopy. Bull. Kor. Chem. Soc. 20, 1021–1025.

Clark, R.N., 1983. Spectral properties of mixtures of montmorillonite and dark carbon grains: implications for remote sensing minerals containing chemically and physically adsorbed water. J. Geophys. Res. Solid Earth 88, 10635–10644. http://dx.doi.org/10.1029/JB088iB12p10635.

Clark, R.N., 1999. Spectroscopy of rocks and minerals, and principles of spectroscopy. In: Rencz, A.N. (Ed.), Manual of Remote Sensing. John Wiley and Sons, New York, pp. 3–58.

Cloutis, E.A., 1989. Spectral reflectance properties of hydrocarbons: remote-sensing implications. Science 245, 165–168. http://dx.doi.org/10.1126/science.245.4914.165.

Cole, M., Lindeque, P., Fileman, E., Halsband, C., Goodhead, R., Moger, J., Galloway, T.S., 2013. Microplastic ingestion by zooplankton. Environ. Sci. Technol. 47, 6646–6655. http://dx.doi.org/10.1021/es400663f.

Colton Jr., J.B., Knapp, F.D., Burns, B.R., 1974. Plastic particles in surface waters of the Northwestern Atlantic. Science 185, 491–497. http://dx.doi.org/10.2307/1738284.

Dierssen, H., McManus, G.B., Chlus, A., Qiu, D., Gao, B.-C., Lin, S., 2015a. Space station image captures a red tide ciliate bloom at high spectral and spatial resolution. Proc. Natl. Acad. Sci. 112, 14783–14787. http://dx.doi.org/10.1073/pnas.1512538112.

Dierssen, H.M., Chlus, A., Russell, B., 2015b. Hyperspectral discrimination of floating mats of seagrass wrack and the macroalgae *Sargassum* in coastal waters of Greater Florida Bay using airborne remote sensing. Remote Sens. Environ. 167, 247–258. http://dx.doi.org/10.1016/j.rse.2015.01.027.

Donohue, J.L., Pavlekovsky, K., Collins, T., Andrady, A.L., Proskurowski, G.K., Law, K.L., 2016. Variability in the composition of floating microplastics by region and in time. In: Ocean Science Meeting Session Abstracts: The emerging science of marine debris: From assessment to knowledge that informs solutions I, pp. 21–26 (New Orleans, Louisiana, USA).

Driedger, A., Dürr, H., Mitchell, K., Flannery, J., Brancazi, E., Van Cappellen, P., 2013. Plastic debris: remote sensing and characterization (Sheboygan, Wisconsin, USA) In: Lake Michigan: State of Lake Michigan and the 13th annual Great Lakes Beach Association Conference, pp. 15–17 (Sheboygan, Wisconsin, USA).

Eerkes-Medrano, D., Thompson, R.C., Aldridge, D.C., 2015. Microplastics in freshwater systems: a review of the emerging threats, identification of knowledge gaps and prioritisation of research needs. Water Res. 75, 63–82. http://dx.doi.org/10.1016/j.watres.2015.02.012.

Eriksen, M., Lebreton, L.C.M., Carson, H.S., Thiel, M., Moore, C.J., Borerro, J.C., Galgani, F., Ryan, P.G., Reisser, J., 2014. Plastic pollution in the world's oceans: more than 5 trillion plastic pieces weighing over 250,000 tons afloat at sea. PLoS One 9, e111913. http://dx.doi.org/10.1371/journal.pone.0111913.

Fazey, F.M.C., Ryan, P.G., 2016. Biofouling on buoyant marine plastics: an experimental study into the effect of size on surface longevity. Environ. Pollut. 210, 354–360. http://dx.doi.org/10.1016/j.envpol.2016.01.026.

Filella, M., 2015. Questions of size and numbers in environmental research on microplastics: methodological and conceptual aspects. Environ. Chem. 12, 527–538. http://dx.doi.org/10.1071/EN15012.

Galgani, F., Hanke, G., Werner, S., De Vrees, L., 2013. Marine litter within the European marine strategy framework directive. ICES J. Mar. Sci. 70, 1055–1064. http://dx.doi.org/10.1093/icesjms/fst122.

Gao, B.-C., Montes, M.J., Ahmad, Z., Davis, C.O., 2000. Atmospheric correction algorithm for hyperspectral remote sensing of ocean color from space. Appl. Opt. 39, 887–896. http://dx.doi.org/10.1364/AO.39.000887.

Garaba, S.P., Dierssen, H.M., 2017. Spectral reference library of 11 types of virgin plastic pellets common in marine plastic debris. Data set available on-line [http://ecosis.org] from the Ecological Spectral Information System (EcoSIS). http://dx.doi.org/10.21232/C27H34.

GESAMP, 2015. Sources, fate and effects of microplastics in the marine environment: a global assessment. In: Kershaw, P.J. (Ed.), (IMO/FAO/UNESCO-IOC/UNIDO/WMO/IAEA/UN/UNEP/UNDP Joint Group of Experts on the Scientific Aspects of Marine Environmental Protection). GESAMP Report and Studies No. 90. International Maritime Organization - London, UK, pp. 96.

Gordon, H.R., Wang, M., 1994. Influence of oceanic whitecaps on atmospheric correction of ocean-color sensors. Appl. Opt. 33, 7754–7763. http://dx.doi.org/10.1364/AO.33.007754.

Hasituya, Chen, Z., Wang, L., Wu, W., Jiang, Z., Li, H., 2016. Monitoring plastic-mulched farmland by Landsat-8 OLI imagery using spectral and textural features. Remote Sens. 8, 353. http://dx.doi.org/10.3390/rs8040353.

Hidalgo-Ruz, V., Gutow, L., Thompson, R.C., Thiel, M., 2012. Microplastics in the marine environment: a review of the methods used for identification and quantification. Environ. Sci. Technol. 46, 3060–3075. http://dx.doi.org/10.1021/es2031505.

Hörig, B., Kühn, F., Oschütz, F., Lehmann, F., 2001. HyMap hyperspectral remote sensing to detect hydrocarbons. Int. J. Remote Sens. 22, 1413–1422. http://dx.doi.org/10.1080/01431160120909.

Hu, C., Feng, L., Hardy, R.F., Hochberg, E.J., 2015. Spectral and spatial requirements of remote measurements of pelagic *Sargassum* macroalgae. Remote Sens. Environ. 167, 229–246. http://dx.doi.org/10.1016/j.rse.2015.05.022.

Huguenin, R.L., Jones, J.L., 1986. Intelligent information extraction from reflectance spectra: absorption band positions. J. Geophys. Res. Solid Earth 91, 9585–9598. http://dx.doi.org/10.1029/JB091iB09p09585.

Huth-Fehre, T., Feldhoff, R., Kantimm, T., Quick, L., Winter, F., Cammann, K., van den Broek, W., Wienke, D., Melssen, W., Buydens, L., 1995. NIR - remote sensing and artificial neural networks for rapid identification of post consumer plastics. J. Mol. Struct. 348, 143–146. http://dx.doi.org/10.1016/0022-2860(95)08609-Y.

Ivar do Sul, J.A., Costa, M.F., 2014. The present and future of microplastic pollution in the marine environment. Environ. Pollut. 185, 352–364. http://dx.doi.org/10.1016/j.envpol.2013.10.036.

Jambeck, J.R., Geyer, R., Wilcox, C., Siegler, T.R., Perryman, M., Andrady, A., Narayan, R., Law, K.L., 2015. Plastic waste inputs from land into the ocean. Science 347, 768–771. http://dx.doi.org/10.1126/science.1260352.

Kanhai, L.D.K., Officer, R., Lyashevska, O., Thompson, R.C., O'Connor, I., 2017. Microplastic abundance, distribution and composition along a latitudinal gradient in the Atlantic Ocean. Mar. Pollut. Bull. 115, 307–314. http://dx.doi.org/10.1016/j.marpolbul.2016.12.025.

Kaynak, C., Sarı, B., 2016. Accelerated weathering performance of polylactide and its montmorillonite nanocomposite. Appl. Clay Sci. 121, 86–94. http://dx.doi.org/10.1016/j.clay.2015.12.025.

Knaeps, E., Ruddick, K.G., Doxaran, D., Dogliotti, A.I., Nechad, B., Raymaekers, D., Sterckx, S., 2015. A SWIR based algorithm to retrieve total suspended matter in extremely turbid waters. Remote Sens. Environ. 168, 66–79. http://dx.doi.org/10.1016/j.rse.2015.06.022.

Koelmans, A.A., Besseling, E., Shim, W.J., 2015. Nanoplastics in the aquatic environment. Critical review. In: Bergmann, M., Gutow, L., Klages, M. (Eds.), Marine Anthropogenic Litter. Eprint ID 37207 of the Alfred-Wegener-Institut Helmholtz-Zentrum für Polar- und Meeresforschung.: Springer International Publishing, pp. 325–340.

Kooi, M., Reisser, J., Slat, B., Ferrari, F.F., Schmid, M.S., Cunsolo, S., Brambini, R., Noble, K., Sirks, L.-A., Linders, T.E.W., Schoeneich-Argent, R.I., Koelmans, A.A., 2016. The effect of particle properties on the depth profile of buoyant plastics in the ocean. Sci. Rep. 6, 33882. http://dx.doi.org/10.1038/srep33882.

Kou, L., Labrie, D., Chylek, P., 1993. Refractive indices of water and ice in the 0.65- to 2.5-μm spectral range. Appl. Opt. 32, 3531–3540. http://dx.doi.org/10.1364/AO.32.003531.

Kühn, F., Oppermann, K., Hörig, B., 2004. Hydrocarbon index – an algorithm for hyperspectral detection of hydrocarbons. Int. J. Remote Sens. 25, 2467–2473. http://dx.doi.org/10.1080/01431160310001642287.

Kutser, T., Miller, I., Jupp, D.L.B., 2006. Mapping coral reef benthic substrates using hyperspectral space-borne images and spectral libraries. Estuar. Coast. Shelf Sci. 70, 449–460. http://dx.doi.org/10.1016/j.ecss.2006.06.026.

Law, K.L., Morét-Ferguson, S., Maximenko, N.A., Proskurowski, G., Peacock, E.E., Hafner, J., Reddy, C.M., 2010. Plastic accumulation in the North Atlantic subtropical gyre. Science 329, 1185–1188. http://dx.doi.org/10.1126/science.1192321.

Lenz, R., Enders, K., Stedmon, C.A., Mackenzie, D.M.A., Nielsen, T.G., 2015. A critical

assessment of visual identification of marine microplastic using Raman spectroscopy for analysis improvement. Mar. Pollut. Bull. 100, 82–91. http://dx.doi.org/10.1016/j.marpolbul.2015.09.026.
Lithner, D., Larsson, Å., Dave, G., 2011. Environmental and health hazard ranking and assessment of plastic polymers based on chemical composition. Sci. Total Environ. 409, 3309–3324. http://dx.doi.org/10.1016/j.scitotenv.2011.04.038.
Mace, T.H., 2012. At-sea detection of marine debris: overview of technologies, processes, issues, and options. Mar. Pollut. Bull. 65, 23–27. http://dx.doi.org/10.1016/j.marpolbul.2011.08.042.
Masoumi, H., Safavi, S.M., Khani, Z., 2012. Identification and classification of plastic resins using near infrared reflectance spectroscopy. World Acad. Sci. Eng. Technol. 6, 141–148.
Masura, J., Baker, J., Foster, G., Courtney, A., Herring, C., 2015. Laboratory methods for the analysis of microplastics in the marine environment: recommendations for quantifying synthetic particles in waters and sediments. In: NOAA Technical Memorandum NOS-OR&R-48. NOAA Marine Debris Division, MD, USA, pp. 39.
Maximenko, N., Arvesen, J., Asner, G., Carlton, J., Castrence, M., Centurioni, L., Chao, Y., Chapman, J., Chirayath, V., Corradi, P., Crowley, M., Dierssen, H.M., Dohan, K., Eriksen, M., Galgani, F., Garaba, S.P., Goni, G., Griffin, D., Hafner, J., Hardesty, D., Isobe, A., Jacobs, G., Kamachi, M., Kataoka, T., Kubota, M., Law, K.L., Lebreton, L., Leslie, H.A., Lumpkin, R., Mace, T.H., Mallos, N., McGillivary, P.A., Moller, D., Morrow, R., Moy, K.V., Murray, C.C., Potemra, J., Richardson, P., Robberson, B., Thompson, R., van Sebille, E., Woodring, D., January 2016. Remote Sensing of Marine Debris to Study Dynamics, Balances and Trends. Honolulu, Hawaii, USA, 19-21 January 2016 In: White Paper from Workshop on Mission Concepts for Marine Debris Sensing, pp. 22 Submitted to Decadal Survey for Earth Science and Applications from Space.
Moller, D., Chao, Y., Maximenko, N., 2016. Remote sensing of marine debris. In: EEE International Geoscience and Remote Sensing Symposium (IGARSS). 36111. pp. 4. http://dx.doi.org/10.1109/IGARSS.2016.7731005. (Beijing, China, 10–15 July 2016).
Moroni, M., Mei, A., Leonardi, A., Lupo, E., Marca, F., 2015. PET and PVC separation with hyperspectral imagery. Sensors 15, 2205. http://dx.doi.org/10.3390/s150102205.
Moses, W.J., Bowles, J.H., Lucke, R.L., Corson, M.R., 2012. Impact of signal-to-noise ratio in a hyperspectral sensor on the accuracy of biophysical parameter estimation in case II waters. Opt. Express 20, 4309–4330. http://dx.doi.org/10.1364/OE.20.004309.
Novelli, A., Tarantino, E., 2015. Combining ad hoc spectral indices based on LANDSAT-8 OLI/TIRS sensor data for the detection of plastic cover vineyard. Remote Sens. Lett. 6, 933–941. http://dx.doi.org/10.1080/2150704X.2015.1093186.
Petropoulos, G.P., Vadrevu, K.P., Kalaitzidis, C., 2013. Spectral angle mapper and object-based classification combined with hyperspectral remote sensing imagery for obtaining land use/cover mapping in a Mediterranean region. Geocarto Int. 28, 114–129. http://dx.doi.org/10.1080/10106049.2012.668950.
Pichel, W.G., Veenstra, T.S., Churnside, J.H., Arabini, E., Friedman, K.S., Foley, D.G., Brainard, R.E., Kiefer, D., Ogle, S., Clemente-Colón, P., Li, X., 2012. GhostNet marine debris survey in the Gulf of Alaska – satellite guidance and aircraft observations. Mar. Pollut. Bull. 65, 28–41. http://dx.doi.org/10.1016/j.marpolbul.2011.10.009.
Reisser, J., Shaw, J., Wilcox, C., Hardesty, B.D., Proietti, M., Thums, M., Pattiaratchi, C., 2013. Marine plastic pollution in waters around Australia: characteristics, concentrations, and pathways. PLoS One 8, e80466. http://dx.doi.org/10.1371/journal.pone.0080466.
Reisser, J., Slat, B., Noble, K., du Plessis, K., Epp, M., Proietti, M., de Sonneville, J., Becker, T., Pattiaratchi, C., 2015. The vertical distribution of buoyant plastics at sea: an observational study in the North Atlantic Gyre. Biogeosciences 12, 1249–1256. http://dx.doi.org/10.5194/bg-12-1249-2015.
Röttgers, R., McKee, D., Utschig, C., 2014. Temperature and salinity correction coefficients for light absorption by water in the visible to infrared spectral region. Opt. Express 22, 25093–25108. http://dx.doi.org/10.1364/OE.22.025093.
Rouse, J.W., Haas, R.H., Schell, J.A., Deering, D.W., 1973. Monitoring vegetation systems in the Great Plains with ERTS. In: Freden, S.C., Mercanti, E.P., Becker, M.A. (Eds.), Third Earth Resources Technology Satellite-1 Symposium: The Proceedings of a Symposium Held by Goddard Space Flight Center, pp. 309–317 (Washington, DC, USA, 10–14 December 1973).
Russell, B., Dierssen, H., LaJeunesse, T., Hoadley, K., Warner, M., Kemp, D., Bateman, T., 2016. Spectral reflectance of Palauan reef-building coral with different symbionts in response to elevated temperature. Remote Sens. 8, 164. http://dx.doi.org/10.3390/rs8030164.
Ryan, P.G., Moloney, C.L., 1993. Marine litter keeps increasing. Nature 361, 23.
Samokhin, A., Sotnezova, K., Lashin, V., Revelsky, I., 2015. Evaluation of mass spectral library search algorithms implemented in commercial software. J. Mass Spectrom. 50, 820–825. http://dx.doi.org/10.1002/jms.3591.
Scafutto, R.D.P.M., de Souza Filho, C.R., de Oliveira, W.J., 2017. Hyperspectral remote sensing detection of petroleum hydrocarbons in mixtures with mineral substrates: implications for onshore exploration and monitoring. ISPRS J. Photogramm. Remote Sens. 128, 146–157. http://dx.doi.org/10.1016/j.isprsjprs.2017.03.009.
Schwarz, J., Staenz, K., 2001. Adaptive threshold for spectral matching of hyperspectral data. Can. J. Remote. Sens. 27, 216–224. http://dx.doi.org/10.1080/07038992.2001.10854938.
van Sebille, E., Wilcox, C., Lebreton, L., Maximenko, N., Hardesty, B.D., van Franeker, J.A., Eriksen, M., Siegel, D., Galgani, F., Law, K.L., 2015. A global inventory of small floating plastic debris. Environ. Res. Lett. 10, 124006. http://dx.doi.org/10.1088/1748-9326/10/12/124006.
SEP, 2011. Plastic waste: Ecological and human health impacts. In: Science for Environment Policy(SEP), In-depth Reports. European Commission's Directorate-General Environment, pp. 44.
Settle, J.J., Drake, N.A., 1993. Linear mixing and the estimation of ground cover proportions. Int. J. Remote Sens. 14, 1159–1177. http://dx.doi.org/10.1080/01431169308904402.
Shah, A.A., Hasan, F., Hameed, A., Ahmed, S., 2008. Biological degradation of plastics: a comprehensive review. Biotechnol. Adv. 26, 246–265. http://dx.doi.org/10.1016/j.biotechadv.2007.12.005.
Shanmugam, S., SrinivasaPerumal, P., 2014. Spectral matching approaches in hyperspectral image processing. Int. J. Remote Sens. 35, 8217–8251. http://dx.doi.org/10.1080/01431161.2014.980922.
Shaw, D.G., Day, R.H., 1994. Colour- and form-dependent loss of plastic micro-debris from the North Pacific Ocean. Mar. Pollut. Bull. 28, 39–43. http://dx.doi.org/10.1016/0025-326X(94)90184-8.
Singh, K.P., 1995. Monitoring of oil spills using airborne and spaceborne sensors. Adv. Space Res. 15, 101–110. http://dx.doi.org/10.1016/0273-1177(95)00080-X.
Slonecker, T., Fisher, G.B., Aiello, D.P., Haack, B., 2010. Visible and infrared remote imaging of hazardous waste: a review. Remote Sens. 2, 2474–2508. http://dx.doi.org/10.3390/rs2112474.
Thevenon, F., Carroll, C., Sousa, J. (Eds.), 2014. Plastic Debris in the Ocean: The Characterization of Marine Plastics and their Environmental Impacts, Situation Analysis Report. International Union for Conservation of Nature, Gland, Switzerland, pp. 52.
Thompson, R.C., Olsen, Y., Mitchell, R.P., Davis, A., Rowland, S.J., John, A.W.G., McGonigle, D., Russell, A.E., 2004. Lost at sea: where is all the plastic? Science 304, 838. http://dx.doi.org/10.1126/science.1094559.
Tsai, F., Philpot, W., 1998. Derivative analysis of hyperspectral data. Remote Sens. Environ. 66, 41–51. http://dx.doi.org/10.1016/S0034-4257(98)00032-7.
USEPA, 2011. Marine Debris in the North Pacific. A Summary of Existing Information and Identification of Data Gaps. U.S. Environmental Protection Agency, San Francisco, USA, pp. 23.
Vázquez-Guardado, A., Money, M., McKinney, N., Chanda, D., 2015. Multi-spectral infrared spectroscopy for robust plastic identification. Appl. Opt. 54, 7396–7405. http://dx.doi.org/10.1364/AO.54.007396.
Verdebout, J., Jacquemoud, S., Andreoli, G., Hosgood, B., Pedrini, A., Schmuck, G., 1995. Analysis of imaging spectrometer data to evaluate the biochemical content of vegetation, based on the results of a laboratory experiment. In: Mougin, E., Ranson, K.J., Smith, J.A. (Eds.), Proceedings of SPIE, Multispectral and Microwave Sensing of Forestry, Hydrology, and Natural Resources. 2314. pp. 14. http://dx.doi.org/10.1117/12.200746. (Rome, Italy, 26–30 September 1994).
Wan, K.X., Vidavsky, I., Gross, M.L., 2002. Comparing similar spectra: from similarity index to spectral contrast angle. J. Am. Soc. Mass Spectrom. 13, 85–88. http://dx.doi.org/10.1016/S1044-0305(01)00327-0.
Wang, J., Kiho, K., Ofiara, D., Zhao, Y., Bera, A., Lohmann, R., Baker, M.C., 2016. Marine debris (chapter 25). In: Inniss, L., Simcock, A. (Eds.), The First Global Integrated Marine Assessment. World Ocean Assessment I: United Nations. 34.
Ward, J.E., Kach, D.J., 2009. Marine aggregates facilitate ingestion of nanoparticles by suspension-feeding bivalves. Mar. Environ. Res. 68, 137–142. http://dx.doi.org/10.1016/j.marenvres.2009.05.002.
Wienke, D., van den Broek, W., Buydens, L., 1995. Identification of plastics among nonplastics in mixed waste by remote sensing near-infrared imaging spectroscopy. 2. Multivariate image rank analysis for rapid classification. Anal. Chem. 67, 3760–3766. http://dx.doi.org/10.1021/ac00116a023.
Zaidi, L., Kaci, M., Bruzaud, S., Bourmaud, A., Grohens, Y., 2010. Effect of natural weather on the structure and properties of polylactide/Cloisite 30B nanocomposites. Polym. Degrad. Stab. 95, 1751–1758. http://dx.doi.org/10.1016/j.polymdegradstab.2010.05.014.